Available online at www.sciencedirect.com
ScienceDirect
Trans. Nonferrous Met. Soc. China 27(2017) 2381−2389
Transactions of Nonferrous Metals Society of China
www.tnmsc.cn

Effects of solid solution treatment and cooling on morphology of LPSO phase and precipitation hardening behavior of Mg−Dy−Ni alloy

Li-tao YUAN[1], Guang-li BI[1], Yuan-dong LI[1], Jing JIANG[1], Yu-xiang HAN[1], Da-qing FANG[2], Ying MA[1]

1. State Key Laboratory of Advanced Processing and Recycling of Non-ferrous Metals, Lanzhou University of Technology, Lanzhou 730050, China;
2. College of Materials Science and Engineering, Taiyuan University of Science and Technology, Taiyuan 030024, China

Received 29 July 2016; accepted 24 February 2017

Abstract: Effects of solid solution treatment and cooling on the morphology of long period stacking order (LPSO) phase and precipitation hardening behavior of Mg−2Dy−0.5Ni (molar fraction, %) alloy were investigated. Microstructures of the as-cast alloy mainly consisted of α-Mg phase, bamboo-like $Mg_{12}DyNi$ phase with LPSO structure distributed between dendrites and small amounts of cubic Dy phases. During solid solution treatment at 565 °C for 12 h and subsequent different cooling conditions, dot-shaped, block, fine lamellar and rod-shaped LPSO phases precipitate in Mg matrix, respectively. For continuous cooling conditions (furnace and air cooling), the fine lamellar LPSO phase generally forms in grain interior and its volume fraction increases and block LPSO phase coarsens with increasing cooling time. For discontinuous cooling conditions (air cooling after furnace cooling to 415 and 265 °C), the dot-shaped LPSO grows into the rod-shaped phase, which results in an decrease of cooling hardening behavior of alloy.

Key words: Mg−Dy−Ni alloy; LPSO phase; microstructure; precipitation hardening

1 Introduction

Magnesium (Mg) alloys are one of the lowest density metal structure materials, and parts of them have been widely applied to the automotive fields due to their high specific stiffness, good damping capacity and machinability [1]. However, poor heat resistance of Mg alloy still limits their development in some industry fields. Thus, it is a significant issue to develop new kinds of heat resistance Mg alloys to expand their application [2−5].

Recently, Mg-based alloys with long-period stacking ordered (LPSO) structures have received considerable interest [6−12]. KAWAMURA et al [6] reported that the tensile yield strength and elongation of a $Mg_{97}Zn_1Y_2$ (molar fraction, %) alloy prepared by rapid solidification processing and hot extrusion can reach 610 MPa and ~5%, respectively. These excellent mechanical properties are manly ascribed to the precipitation of dispersed nano-scale LPSO phases [7]. The LPSO phase has a high thermal stability and good coherent interface with α-Mg matrix. Furthermore, the morphology, distribution, scale, volume fraction and structure of LPSO phase determine the heat resistance of alloy. At present, alloying, heat treatment and hot working could effectively modify the above properties of LPSO phase [13−16]. LIU et al [13] investigated that the addition of Zn effectively increased the volume fraction of LPSO phase in extruded Mg−5Y−4Gd−0.4Zr alloy. This phase plays an important role in improving the mechanical properties, especially for the elongation of alloy. WANG et al [14] found that the volume fraction of the LPSO phase of the $Mg_{94}Zn_{2.5}Y_{2.5}Mn_1$ alloy reached a peak (24.8%) with addition of 0.34% (molar fraction) Ca and the alloy exhibited an ultimate tensile strength of 231 MPa and a elongation of 8.6%, respectively. Additionally, ZHANG et al [15] reported that the block 18R-LPSO phase at the grain boundary transforms to 14H-LPSO phase in the grain interior for

Foundation item: Projects (51301082, 51464031) supported by the National Natural Science Foundation of China; Project (2015011038) supported by the Natural Science Foundation of Shanxi Province, China
Corresponding author: Guang-li BI; Tel/Fax: +86-931-2973564; E-mail: glbi@163.com
DOI: 10.1016/S1003-6326(17)60264-4

$Mg_{93.83}Zn_{1.5}Dy_{4.5}Zr_{0.17}$ alloy during aging-treatment and the tensile strength and elongation of the aging-treated alloy are 253 MPa and 10.5%, respectively. In addition, LU et al [16] demonstrated that the block, lamellar, and rod-shaped LPSO phase of $Mg_{95.2}Zn_2Y_{2.7}$ alloy could be obtained respectively by annealing heat treatment and the block LPSO phases are more conductive to the strength of the alloy. Additionally, hot working could refine LPSO phase and make the LPSO phase transform from 18R to 14H type, such as extrusion [17], hot rolling [18] and forging [19].

Previous literatures [16,20] have demonstrated that annealing heat treatment could obtain different morphology LPSO phases in Mg−Zn−Y alloys. However, the effect of continuous and discontinuous cooling on the morphology LPSO phase for Mg−Dy−Ni alloy has less been studied until now. At present, we have investigated the microstructure and mechanical properties of as-cast Mg−Dy−Ni alloy [21]. Therefore, in this work, the microstructure evolution and precipitation hardening behavior of the alloy during cooling were investigated. The transformation mechanism of morphology of LPSO phase during cooling was discussed.

2 Experimental

Mg−2Dy−0.5Ni (molar fraction, %) alloy was prepared from high pure Mg and Ni and Mg−20Dy (mass fraction, %) master alloy. Melting was conducted by using a graphite crucible in an electric resistance furnace at about 750 °C under the protection of antioxidant flux. The melts were homogenized at 720 °C for 0.5 h, and then cast into a steel mould with size of 70 mm × 40 mm × 13 mm. The specimens for solid-solution treatment were cut from the bulk as-cast ingot with size of 10 mm × 10 mm × 5 mm. The specimens were solution treated at 565 °C for 12 h in box resistance furnace of SX2-4-10 style and then quenched into water at room temperature. Then, the specimens after solid-solution treatment at 565 °C for 12 h were cooled at different cooling conditions which consist of air cooling after solid solution heat-treated state (S+A), furnace cooling after solid solution heat-treated state (S+F), air cooling after furnace cooling to 415 °C (S+415F+A) and cooling after furnace cooling to 265 °C (S+265F+A).

Microstructure, phase structure and phase composition of the alloy were characterized using optical microscopy (Olympus GX71), X-ray diffractometry (XRD) (Rigaku D/max 2500 PC), scanning electron microscopy (EDS) and transmission electronic microscopy (TEM) (JEM-2100F). Calorimetric response of the as-cast alloy was measured using differential scanning calorimetry (DSC). Specimens for microstructure observations were firstly ground on 400#, 600#, 800# and 1000# silicon carbide papers and etched after polishing in a solution of picric and 2% nitric acid. Phase analysis was conducted using X-ray diffractometer (XRD) with a copper target at scanning angles from 20° to 80° and scanning speed of 1.2 (°)/min. The thin foils with a diameter of 3 mm for the TEM observation were prepared using ion polishing system (RES101). The volume fraction of LPSO phase was measured by using Image-Pro Plus 6.0 and at least five OM/SEM images were analyzed for each state. Vickers hardness was measured by hardness tester (HV-100) with a load of 1 N, a dwelling time of 15 s and 10 measurements were collected for each sample.

3 Results and discussion

3.1 Microstructure of alloy in as-cast and solution heat-treated states

Figure 1 shows the DSC curve of as-cast alloy. The DSC heating curve contains two endothermic peaks. One peak is 570.2 °C which is close to the temperature of formation of the second phases. The other is at 600.2 °C which is close to the melting temperature of α-Mg according to the equilibrium phase diagram of the Mg−Dy alloy [22]. Therefore, the solution heat treatment of alloy was selected as 565 °C.

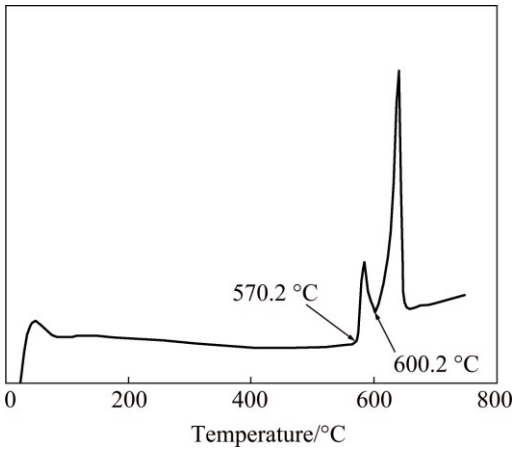

Fig. 1 DSC curve of alloy

The as-cast alloy is mainly composed of black α-Mg dendrites and second phases between dendrites, as shown in Fig. 2(a). These second phases are mainly composed of bamboo-like phase and a small amount of the square particle phases. EDS analysis results in Table 1 reveal that chemical compositions of black dendrites (point *A* in Fig. 2(a)), bamboo-like phase (point *B* in Fig. 2(a)) and cubic particle phase (point *C* in Fig. 2(a)) are Mg99.3−Dy0.7, Mg92.6−Dy4.4−Ni3.0 and Mg31.2−Dy66.5−Ni2.3 (molar fraction, %), respectively. According to previous investigation [21] and XRD results (Fig. 3),

the bamboo-like phase is $Mg_{12}NiDy$ with an 18R-type LPSO structure. The phase has an hcp structure and its lattice constants are a=0.321 nm and c=4.86 nm. The $Mg_{12}NiDy$ phase has a similar crystalline structure with the $Mg_{12}ZnDy$ phase in the as-cast $Mg_{97.5}Zn_{0.5}Dy_2$ alloy [23] and the $Mg_{12}ZnY$ phase in $Mg_{97}Zn_1Y_2$ alloy [13,24], respectively. The cubic particle phase is a Dy phase [21]. The Dy phase is not detected in the XRD pattern in Fig. 3 due to small amount.

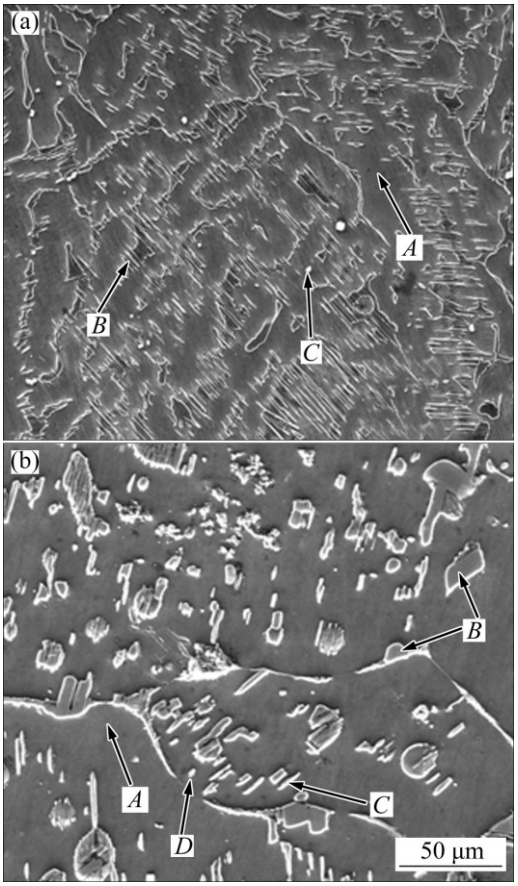

Fig. 2 SEM images of alloy in as-cast state (a) and solid solution heat-treated state at 565 °C for 12 h (b)

Table 1 EDS analysis results of phases in Fig. 2(a)

Position	x/%		
	Mg	Dy	Ni
A	99.3	0.7	0.0
B	92.6	4.4	3.0
C	31.2	66.5	2.3

Figure 2(b) shows SEM image of the alloy in solution heat-treated state at 565 °C for 12 h. The alloy in solution heat-treated state is mainly composed of black matrix phase, block phase, dot-shaped phase and square particle phase. The EDS analysis result in Table 2 reveals that black matrix phase is α-Mg matrix (point *A* in Fig. 2(b)). The round block phase randomly distributed in the grain interior (point *B* in Fig. 2(b)) and the web-like block phase in the grain boundary are LPSO phases with an 18R-type LPSO structure, which are transformed from bamboo-like LPSO phase in as-cast alloy [25]. The phase precipitates as a continuous web structure at the grain boundaries. The chemical composition of dot-shaped phase is Mg87.2−Dy6.7−Ni6.1, which is close with that of 14H type LPSO structure in the heat-treated $Mg_{97}Y_2Zn_1$ alloy [20]. The precipitation of 14H type LPSO phase in α-Mg supersaturated solid solution mainly contains two processes. One is the diffusion of Dy and Ni atoms from α-Mg supersaturated solid solution to the ordered stacking faults region. The other is the formation of ordered stacking faults due to addition of Dy and Ni atoms. The LPSO phase precipitates when the above two conditions are simultaneously met. The formation mechanism has been reported in other Mg alloys [26,27]. A small amount of white cubic particle phases (point *D* in Fig. 2(b)) are undissolved Dy phases in Mg matrix. This indicates that the phase has a high thermal stability.

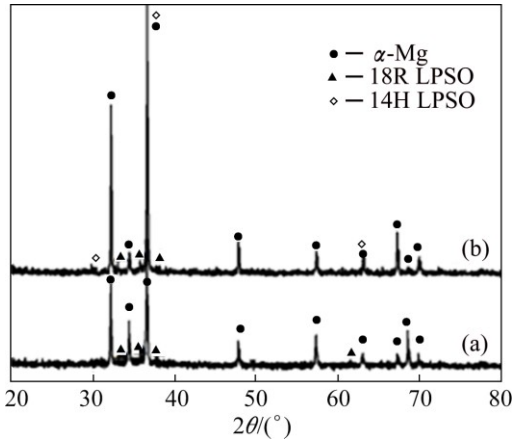

Fig. 3 XRD patterns of alloy in as-cast state (a) and solution heat-treated state at 565 °C for 12 h (b)

Table 2 EDS analysis results of phases in Fig. 2(b)

Position	x/%		
	Mg	Dy	Ni
A	98.9	1.0	0.1
B	90.5	5.5	4.0
C	87.2	6.7	6.1
D	55.6	43.3	1.1

3.2 Microstructure evolution of alloy under different cooling conditions

Figure 4 shows optical and SEM images of the alloy under continuous cooling condition after 565 °C for 12 h. Owing to different cooling rates, significant change in microstructure of alloy occurs. For S+A, it can be seen in Fig. 4(c) and Fig. 4(d) that the web-like block phase and

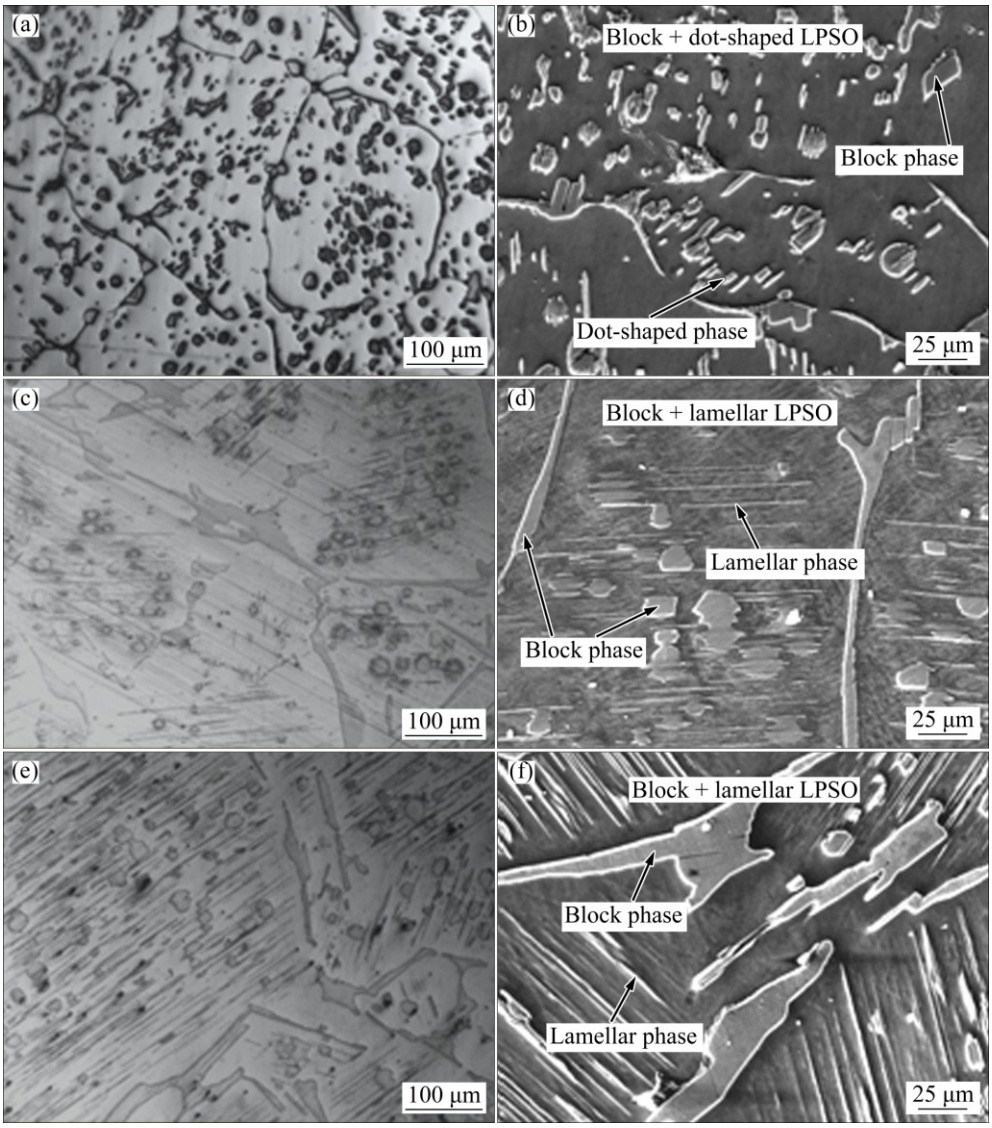

Fig. 4 Optical and SEM images of alloy in different continuous cooling conditions: (a, b) Solid solution at 565 °C for 12 h; (c, d) S+A; (e, f) S+F

round block phase coarsen, meanwhile, the new fine lamellar LPSO phase forms in the Mg matrix. The chemical composition of the fine lamellar phase is Mg91.2−Dy5.2−Ni3.6 (molar fraction, %) in Table 3. The content ratio of Dy/Ni is close to that of Dy/Zn of LPSO phase in Mg−Dy−Zn alloy [28] with a 14H LPSO structure. So, the lamellar phase has a 14H LPSO structure, which is consistent with the XRD pattern shown in Fig. 5. The fine lamellar phase appears due to two reasons. One is the growth of dot-shaped phases and the other is the precipitation of the supersaturated α-Mg matrix during cooling process. Moreover, all the fine lamellar phases in each grain have the same direction. For S+F, it can be seen in Fig. 4(e) and Fig. 4(f) that there is no other phase observed compared to the alloy under S+A. With cooling rate of alloy decreasing, Dy and Ni elements diffuse sufficiently. As a result, both the block phases and lamellar phases of the alloy coarsen obviously and the volume fraction of fine 14H LPSO phase increases. The decrease in continuous cooling rate is helpful to the precipitation of a fine 14H LPSO phase within α-Mg grain [29]. The schematic diagram of morphology evolution of LPSO phase for alloy under continuous cooling process is shown in Fig. 6(a), which clearly indicates the precipitation process of lamellar 14H LPSO phase.

Table 3 EDS analysis results of lamellar phase and rod-shaped phase

Phase	x/%		
	Mg	Dy	Ni
Lamellar phase	91.2	5.2	3.6
Rod-shaped phase	88.1	6.8	5.1

Figure 7 shows optical and SEM images of the alloy under discontinuous cooling condition after solid

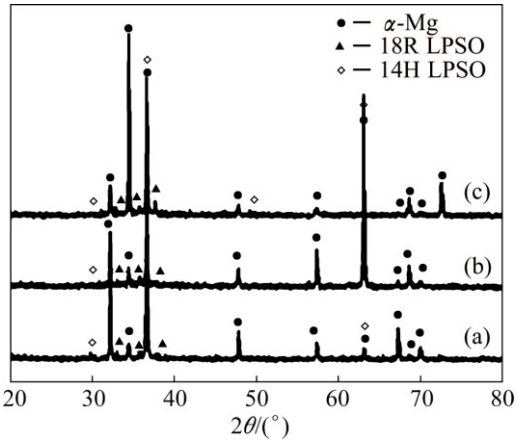

Fig. 5 XRD patterns of alloy in different continuous cooling conditions: (a) Solid solution at 565 °C for 12 h; (b) S+A; (c) S+F

solution at 565 °C for 12 h. For S+415F+A, it can be seen in Fig. 7(c) and Fig. 7(d) that the block LPSO phase appears from continuous to discontinuous distribution in the Mg matrix. It can be seen in Table 3 that a rod-shape phase forms and its composition is Mg88.1−Dy6.8−Ni5.1 (molar fraction, %) where Dy/Ni content ratio is 4/3, which is close to Y/Zn content ratio of LPSO phase in Mg−Y−Zn alloy [16]. There are still diffraction peaks of 14H LPSO phase of the alloy without dot-shaped phase under discontinuous cooling in Fig. 8. Thus, the rod-shape phase is determined to have a 14H LPSO structure. The precipitation of rod-shape LPSO phase arises from the growth of dot-shape LPSO phase. For S+265F+A, the block LPSO phase and precipitation of rod-shape LPSO phase still exist, while the two phases coarsen as compared to S+415F+A. It is noted that the volume fraction of rod-shaped LPSO phase increases while that of block LPSO phase decreases, as shown Fig. 9. That indicates that some block phases transform to rod-shaped phases in cooling process. The detail distribution and coarsening processes of LPSO phase are shown in Fig. 6(b). In addition, the TEM images and fast Fourier transformation (FFT) diffraction patterns of LPSO phase of S+415F+A are shown in Fig. 10, where the spacing between the fringes of lattice is 1.6 nm and 1.8 nm in the 18R and 14H LPSO structures, as shown in Figs. 10(b) and (d), respectively. FFT diffraction patterns of block and rod-shaped LPSO phase show that there are six extra diffraction spots at the intervals between $(000)_{18R}$ and $(0018)_{18R}$ spots and seven extra diffraction spots at the intervals between $(000)_{14H}$ and $(0014)_{14H}$ spots. This also indicates that the block phase and rod-shaped LPSO phase in the alloy are 18R and 14H type LPSO structure, respectively, which is consistent with the previous report [9,30].

3.3 Cooling hardening behavior

Figure 11 shows hardness of the alloy in different cooling conditions after solid solution at 565 °C for 12 h. It can be seen that the hardness values of alloy vary with different cooling conditions. The initial hardness value of alloy in solid solution is HV 65. The hardness value of alloy at continuous cooling and S+415F+A decreases slowly, while S+265F+A decreases remarkably to HV 56. The hardness value (HV 56) of alloy is decreased by 14% as compared with that (HV 65) of alloy in solid solution. The difference in hardness value of alloy under different states is mainly attributed to strengthening of LPSO phase and solid solution strengthening. The morphology, scale, distribution and structure of LPSO phase also affect their strengthening role. The above microstructure analysis demonstrates that LPSO has

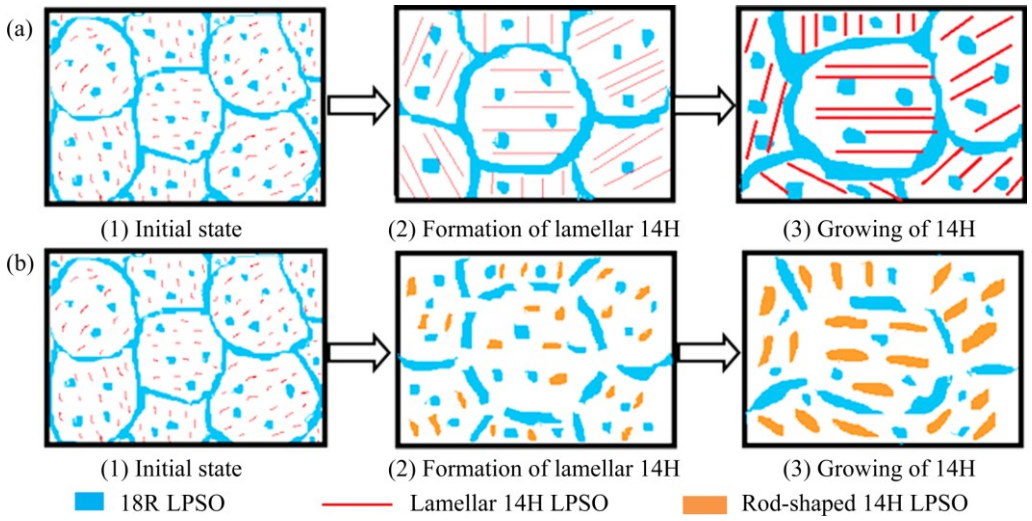

Fig. 6 Schematic diagrams of precipitation behavior of 14H LPSO phase of alloy after solid solution at 565 °C for 12 h: (a) Continuous cooling; (b) Discontinuous cooling

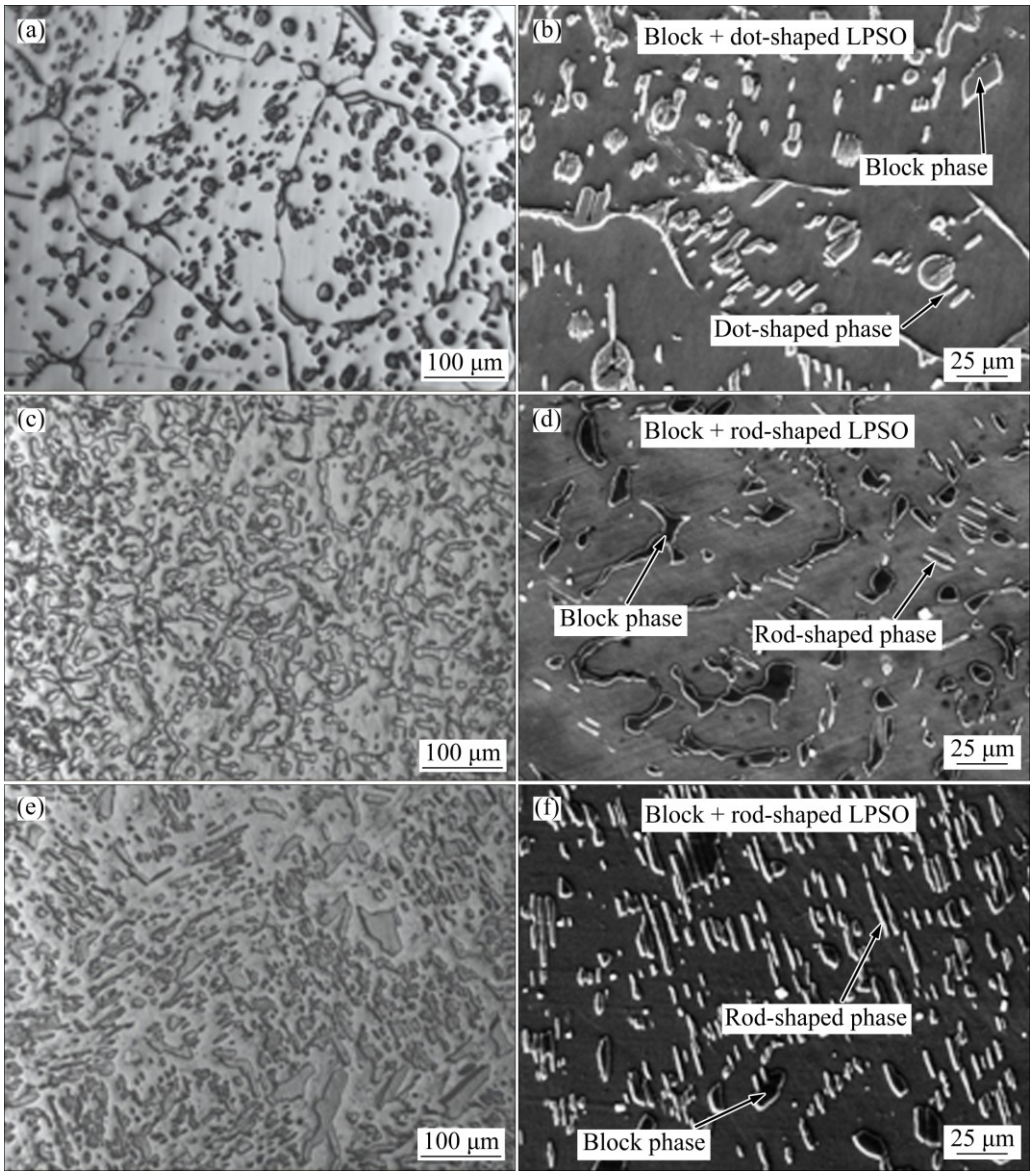

Fig. 7 Optical and SEM images of alloy in different discontinuous cooling conditions; (a, b) Solid solution at 565 °C for 12 h; (c, d) S+415F+A; (e, f) S+265F+A

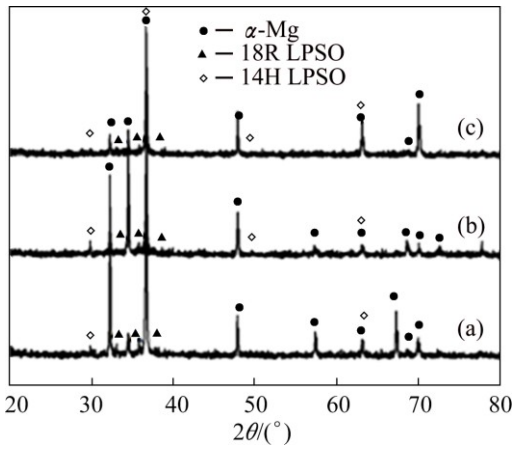

Fig. 8 XRD patterns of alloy in different discontinuous cooling conditions: (a) Solid solution at 565 °C for 12 h; (b) S+415F+A; (c) S+265F+A

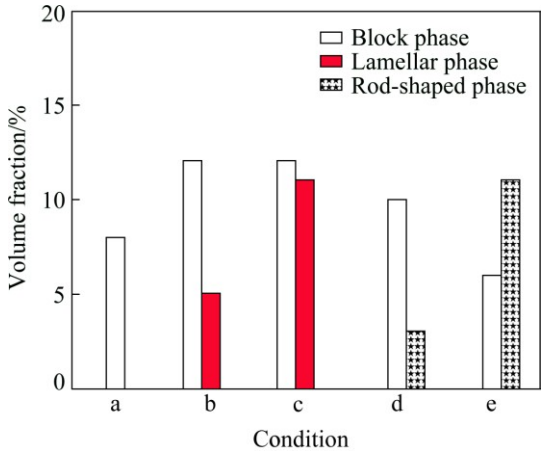

Fig. 9 Volume fraction of various LPSO phases of alloy after solid solution at 565 °C for 12 h (a) under different cooling conditions: (b) S+A; (c) S+F; (d) S+415F+A; (e) S+265F+A

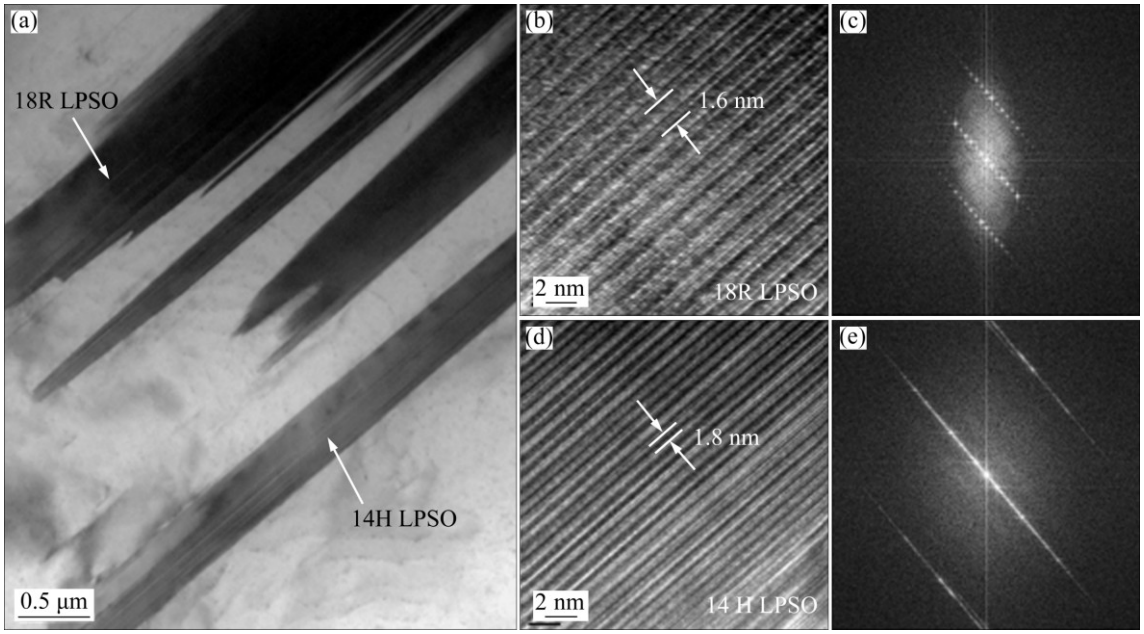

Fig. 10 TEM image (a) and fast Fourier transformation diffraction patterns of LPSO phase of S+415F+A: (b, c) Block phase; (d, e) Rod-shaped phase

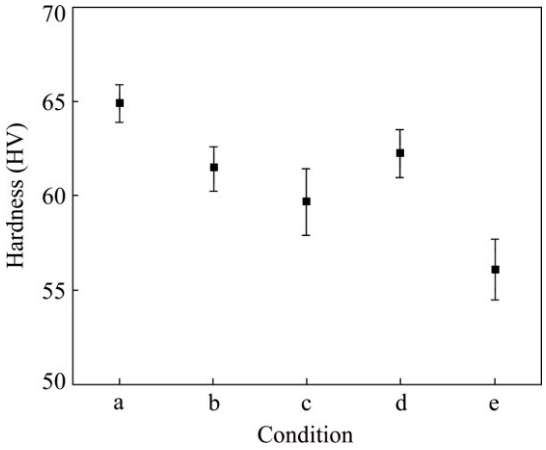

Fig. 11 Microhardness of alloy after solid solution at 565 °C for 12 h (a) under different cooling conditions: (b) S+A; (c) S+F; (d) S+415F+A; (e) S+265F+A

appears three kinds of morphologies and an hcp crystalline structure in different cooling conditions. Three kinds of morphologies of LPSO phase is block, lamellae and rod-shape, respectively. The previous literatures reveled that the precipitation of block LPSO phase at grain boundary and lamellar LPSO phase in grain interior could efficiently improve mechanical properties of alloy by hindering the dislocation movements [31], and in contrast, the formation of rod-shaped LPSO phase deteriorates the strength of alloy due to the poor coherent interface with α-Mg matrix [16]. For the alloys under continuous cooling, only the block and lamellar LPSO phases precipitate and the volume faction of lamellar LPSO phase under S+F is higher than that under S+A. However, the hardness value of alloy under S+F is indeed slightly lower as compared with that of alloy under S+A. This is probably related to the coarsening of LPSO phase during long time furnace cooling. Thus, the hardness value of alloy under S+A is slightly higher than that of alloy under S+F. For the alloys under discontinuous cooling, besides of block LPSO phase, the rod-shaped LPSO phase forms and the volume fraction of this phase increases with decreasing cooling rate. The precipitation of a large amount of rod-shaped LPSO phases leads to the lower hardness value of S+265F+A.

4 Conclusions

1) The alloy in as-cast state is mainly composed of α-Mg dendrites, bamboo-like LPSO phase distributed between dendrites and small amounts of cubic Dy phase. After solid solution heat treatment, bamboo-like LPSO phase transforms into block LPSO phase and dot-shaped LPSO phase.

2) Under continuous cooling, block LPSO phase coarsens and the lamellar LPSO phase generally precipitates in α-Mg matrix and the volume fraction of the phase increases from 5% in air cooling to 11% in furnace cooling. During discontinuous cooling, block LPSO phase appears from continuous to discontinuous distribution in the Mg matrix and rod-shaped LPSO phase forms and its volume fractions under air cooling after furnace cooling to 415 and 265 °C are 3% and 11%, respectively.

3) The hardness of alloy under air cooling after furnace cooling to 415 °C exhibits the highest value of HV 62. The high hardness of alloy is mainly attributed to block LPSO phase strengthening, while the lowest hardness (HV 56) of alloy under air cooling after furnace cooling to 265 °C arises from the precipitation of rod-shaped LPSO phase.

References

[1] ZHANG Ding-fei, SHEN Xia, PAN Fu-sheng, JIANG Lu-yao, HU Guang-shan, YU Da-liang. Research progress of the effect of rare earth elements on mechanical properties of magnesium alloys [J]. Functional Materials, 2014, 45(5): 05001−05007.

[2] LI Ji-lin, CHEN Rong-shi, KE Wei. Microstructure and mechanical properties of Mg−Gd−Y−Zr alloy cast by metal mould and lost foam casting [J]. Transactions of Nonferrous Metals Society of China, 2011, 21(4): 761−766.

[3] YANG Ming-bo, QIN Cai-yuan, PAN Fu-sheng, ZHOU Tao. Comparison of effects of cerium, yttrium and gadolinium additions on as-cast microstructure and mechanical properties of Mg−3Sn−1Mn magnesium alloy [J]. Journal of Rare Earths, 2011, 29(6): 550−557.

[4] ZHANG Kui, LI Xing-gang, LI Yong-jun, MA Ming-long. Effect of Gd content on microstructure and mechanical properties of Mg−Y−RE−Zr alloys [J]. Transactions of Nonferrous Metals Society of China, 2008, 18(S): s12−s16.

[5] LIU Xi-bo, GUAN Xun, CHEN Rong-shi, HAN En-hou. Creep behavior of ageing hardened Mg−10Gd−3Y alloy [J]. Transactions of Nonferrous Metals Society of China, 2010, 20(S): s545−s549.

[6] KAWAMURA Y, HAYASHI K, INOUE A, MASUMOTO T. Rapidly solidified powder metallurgy $Mg_{97}Zn_1Y_2$ alloy with excellent tensile yield strength above 600 MPa [J]. Materials Transactions, 2001, 42(7): 1172−1176.

[7] ABE E, KAWAMURA Y, HAYASHI K, INOUE A. Long-period ordered structure in a high-strength nanocrystalline Mg−1at% Zn−2at% Y alloy studied by stomic-resolution Z-contrast stem [J]. Acta Materialia, 2002, 50(15): 3845−3857.

[8] INOUE A, KAWAMURA Y, MATSUSHITA M, HAYASHI K, KOIKE J. Novel hexagonal structure and ultrahigh strength of magnesium solid solution in the Mg−Zn−Y system [J]. Journal of Materials Research, 2001, 16(7): 1894−1900.

[9] ZHU Y M, MORTON A J, NIE J F. The 18R and 14H long-period stacking ordered structures in Mg−Y−Zn alloys [J]. Acta Materialia, 2010, 58(8): 2936−2947.

[10] ITOI T, SEIMIYA T, KAWAMURA Y, HIROHASHI M. Long period stacking structure observed in $Mg_{97}Zn_1Y_2$ alloy [J]. Scripta Materialia, 2004, 51(2): 107−111.

[11] YAMASAKI M, ANAN T, TOSHIMOTO S, KAWAMURA Y. Mechanical properties of warm-extruded Mg−Zn−Gd alloy with coherent 14H long periodic stacking ordered structure precipitate [J]. Scripta Materialia, 2005, 53(7): 799−803.

[12] YAMASAKI M, SASAKI M, NISHIJIMA M, HIRAGA K, KAWAMURA Y. Formation of 14H long period stacking ordered structure and profuse stacking faults in Mg−Zn−Gd alloys during isothermal aging at high temperature [J]. Acta Materialia, 2007, 55(20): 6798−6805.

[13] LIU Ke, ZHANG Jing-huai, TANG Ding-xiang, ROKHLIN L L, ELKIN F M, MENG Jian. Precipitates formed in a Mg−7Y−4Gd−0.5Zn−0.4Zr alloy during isothermal ageing at 250 °C [J]. Materials Chemistry and Physics, 2009, 117: 107−112.

[14] WANG Jie, ZHANG Jin-shan, ZONG Xi-mei, XU Chun-xiang, YOU Zhi-yong. Effects of Ca on the formation of LPSO phase and mechanical properties of Mg−Zn−Y−Mn alloy [J]. Materials Science and Engineering A, 2015, 648: 37−40.

[15] ZHANG Jin-shan, XIN Chao, NIE Kai-bo, CHENG Wei-li, WANG Hong-xia, XU Chun-xiang. Microstructure and mechanical properties of Mg−Zn−Dy−Zr alloy with long-period stacking ordered phases by heat treatments and ECAP process [J]. Materials Science and Engineering A, 2014, 611: 108−113.

[16] LU Ruo-peng, WANG Jing-feng, CHEN Yong-liang, QIN De-zhao, YANG Wen-xiang, WU Zhong-shan. Effect of heat treatment on the morphology of long-period stacking ordered phase, the corresponding damping capacities and mechanical properties of Mg−Zn−Y alloys [J]. Journal of Alloys and Compounds, 2015, 639: 541−546.

[17] BI Guang-li, LI Yuan-dong, HUANG Xiao-feng, CHEN Ti-jun, LIAN Jian-she, JIANG Zhong-hao, MA Ying, HAO Yuan. Deformation behavior of an extruded Mg−Dy−Zn alloy with long period stacking ordered phase [J]. Materials Science and Engineering A, 2015, 622: 52−60.

[18] ZHENG Liang, LIU Chu-ming, JIN Jin, WANG Xiao, JI Da-wei. Effect of hot-rolling on microstructures and mechanical properties of extruded Mg−6Gd−3.2Y−*x*Zn−o.5Zr sheet [J]. Journal of Materials Engineering and Performance, 2013, 22: 104−111.

[19] NODA M, MATSUMOTO R, KAWAMURA Y. Forging induces changes in the formability and microstructure of extruded $Mg_{96}Zn_2Y_2$ alloy with a long-period stacking order phase [J]. Materials Science and Engineering A, 2013, 563: 21−27.

[20] LIU Huan, BAI Jing, YAN Kai, YAN Jing-li, MA Ai-bin, JIANG Jing-hua. Comparative studies on evolution behavior of 14H LPSO precipitates in as-cast and as-extruded Mg−Y−Zn alloys during annealing at 773 K [J]. Materials and Design, 2016, 93: 9−18.

[21] BI Guang-li, LUO Xiao-mei, JIANG Jing, ZHANG Yong-gang, XU Jian-ji, CHEN Jie-ming, LI Yuan-dong, MA Ying. Effect of Zn, Cu and Ni addition on microstructure and mechanical properties of as-cast Mg−Dy alloy [J]. China Foundry, 2016, 13(1): 54−58.

[22] ZHANG Fan, BI Guang-li, LI Yuan-dong, LI Ming, MA Ying. Effect of solution treatment on microstructure and corrosion properties of Mg−Dy−Zn alloy [J]. Transactions of Materials and Heat, 2015, 36(4): 85−92.

[23] BI Guang-li, LI Yuan-dong, HUANG Xiao-feng, CHEN Ti-jun, MA Ying, HAO Yuan. Dry sliding wear behavior of an extruded Mg−Dy−Zn alloy with long period stacking ordered phase [J]. Journal of Magnesium Alloy, 2015, 3: 63−69.

[24] HAGIHARA K, YOKOTANI N, UMAKOSHI Y. Plastic deformation behavior of $Mg_{12}YZn$ with 18R long-period stacking ordered structure [J]. Intermetallics, 2010, 18: 267−276.

[25] ZHANG Jin-shan, XIN Chao, CHENG Wei-li, BIAN Li-ping, WANG Hong-xia, XU Chun-xiang. Research on long-period-stacking-ordered in Mg−Zn−Dy−Zr alloy [J]. Journal of Alloys and Compounds, 2013, 558: 195−202.

[26] WU Yu-juan, ZENG Xiao-qin, LIN Dong-liang, PENG Li-ming, DING Wwen-jiang. The microstructure evolution with lamellar 14H-type LPSO structure in an Mg96.5Gd2.5Zn1 alloy during solid solution heat treatment at 773 K [J]. Journal of Alloys and Compounds, 2009, 477:193−197.

[27] DING Wen-jiang, WU Yu-juan, PENG Li-ming, ZENG Xiao-qin, YUAN Guang-yin, LIN Dong-liang. Formation of 14H-type long period stacking ordered structure in the as-cast and solid solution treated Mg−Gd−Zn−Zr alloys [J]. Materials Research Society, 2009, 24(5): 1842−1854.

[28] BI Guang-li, FANG Da-qing, ZHAN Lei, ZHANG Qing-xin, LIAN Jian-she, JIANG Qing, JIANG Zhong-hao. Double-peak ageing behavior of Mg−2Dy−0.5Zn alloy [J]. Journal of Alloys and Compounds, 2011, 509: 8286−8275.

[29] QIN De-zhao, WANG Jing-feng, LU Ruo-peng, CHEN Yong-liang, MA She, PAN Fu-sheng. Effects of heat treatment on the morphology of long-period stacking ordered phase and the corresponding damping capacities of Mg−Cu−Zn−Y alloys [J]. Materials Transactions, 2015, 12(12): 2042−2046.
[30] ZHU Y M, WEYLAND M, MORTON A J, OH-ISHI K, HONO K, NIE J F. The building block of long-period structures in Mg−RE−Zn alloys [J]. Scripta Materialia, 2009, 60: 980−983.
[31] SHAO Xiao-hong, YANG Zhi-qing, MA Xiu-liang. Strengthening and toughening mechanisms in Mg−Zn−Y allou with a long period stacking ordered structure [J]. Acta Materialia, 2010, 58(14): 4760−4771.

固溶和冷却处理对 Mg−Dy−Ni 合金中长程堆垛有序(LPSO)相形貌及析出硬化行为的影响

袁利桃[1]，毕广利[1]，李元东[1]，姜 静[1]，韩宇翔[1]，房大庆[2]，马 颖[1]

1. 兰州理工大学 省部共建有色金属先进加工与再利用国家重点实验室，兰州 730050；
2. 太原科技大学 材料科学与工程学院，太原 030024

摘 要：研究了固溶和冷却处理对 Mg−2Dy−0.5Ni(摩尔分数，%)合金中的长程堆垛有序(LPSO)相形貌及析出硬化行为的影响。铸态合金组织主要包括 α-Mg 相、分布在枝晶间具有 LPSO 结构的竹尖状 $Mg_{12}DyNi$ 相和少量立方体状的 Dy 相。在 565 °C 固溶处理 12 h 及随后不同的冷却过程中，点状、块状、细薄片状和棒状的 LPSO 相分别在基体中析出。在连续冷却(空冷和炉冷)的条件下，细薄片状的 LPSO 相逐渐在晶粒内部析出；随着冷却时间的延长，其体积分数亦增加，且块状的 LPSO 相发生粗化。在不连续冷却(炉冷到 415 °C+空冷和炉冷到 265 °C+空冷)条件下，点状 LPSO 相生长成棒状相，降低了合金的冷却硬化作用。

关键词：Mg−Dy−Ni 合金；LPSO 相；显微组织；析出硬化

(Edited by Bing YANG)